OSCILLATION IN THE FLOW OF A POLYMER MELT FROM A CAPILLARY

A. V. Karakin and A. I. Leonov

Zhurnal Prikladnoi Mekhaniki i Tekhnicheskoi Fiziki, Vol. 9, No. 3, pp. 110-114, 1968

A theory is presented for polymer flow that is in qualitative agreement with experiment. The theory is based on the fact [1, 2] that the flow rate does not have a single-valued relation to the pressure difference, as well as on the compressibility of the polymer, which appears very prominently in the source vessel.

There is a fairly extensive body of literature on melt fracture, in which the polymer emerging from the capillary ceases to be smooth at pressure differences above some critical value.

There are several experimental studies [1-3] that give a clear qualitative picture of the effect for certain particular cases. These tests were performed under isothermal conditions with a constant-flow viscometer, which is an axially symmetric system of cylinders joined in series (a large reservoir of radius R and length L, together with a small capillary of radius a and length l, with $a \ll R$ and $l \ll L$). A piston moves at a constant speed U into the reservoir. The pressure at the capillary inlet and the polymer flow rate are measured as functions of time. The melt emerges in jerks for some range $U_1 < U < U_2$, and the recorded pressure varies at the same time; the extruded material shows obvious changes in diameter.

Figure 1 shows the integral flow curve for a capillary viscometer [1-3], in which $\tau = pa/2l$ is the shear stress at the capillary wall, $\dot{\gamma} = 4Q/\pi a^3$ is the mean integral shear rate in the capillary, p is the pressure at the capillary inlet (less atmospheric pressure), and Q is the volume flow rate. The plot of τ against $\dot{\gamma}$ in Fig. 1 is essentially the flow rate against pressure for a given material and capillary. The range $\dot{\gamma}_1$ to $\dot{\gamma}_2$ constitutes one to two orders of magnitude in $\dot{\gamma}$ for a polymer, whereas the range from τ_1 to τ_2 is around 10% of τ_2. This hysteresis region on the curve can thus be overlooked, although a "horizontal" region may be noted.

The hysteresis is often ascribed to slip of the melt along the capillary wall. A simple analysis gives the following relation of $\dot{\gamma}$ to τ, the slip rate $u(\tau)$, and the flow function $f(\tau)$, which defines the non-Newtonian behavior (T is temperature):

$$\dot{\gamma} = \frac{4}{a}u(\tau, T) + \frac{4}{\tau^3}\int_0^\tau f(x, T)\,x^2dx = \dot{\gamma}_s + \dot{\gamma}_m. \qquad (1)$$

Formula (1) may be used by varying a with τ = const to distinguish the shear speed $\dot{\gamma}_m$ from the speed $\dot{\gamma}_s$ due to wall slip. It is found [2] that $\dot{\gamma}_s$ can account for 70-80% of $\dot{\gamma}$, so wall slip dominates the oscillation mechanism* [4]. Use of graphite capillaries [5] also confirms wall slip, as the extruded material is streaked with graphite. The maximum in $\tau(\dot{\gamma})$ is readily explained, as it is entirely due to a maximum in $\tau(u)$, which is familiar from the theory of friction of highly elastic materials. A molecular model has been proposed [6] for such friction. Here we take $\tau(\dot{\gamma})$ as given.

It has also been stated [4] that the $\tau(\dot{\gamma})$ curve (Fig. 1) is almost independent of the absolute hydrostatic pressure, which at first sight conflicts with known relationships to the normal pressure for the friction of highly elastic materials. However, the relationship for solid polymers is due to increase in the area of actual contact as the normal pressure increases. A polymer flowing as a liquid has an actual area of contact almost equal to the area of nominal contact, which explains why the parameters of the wall slip are independent of the hydrostatic pressure.

Tests have been performed [3] with molten high-density polyethylenes of various molecular-weight distributions. As $\langle M_w\rangle / \langle M_n\rangle = k$ increases, where M_w is the weight mean of the molecular weight and M_n is the number mean, the section abcd in Fig. 1 decreases in size, and it is not experimentally detectable for $k > 30$. As k is a measure of the width of the molecular-weight distribution [7], this shows that the maximum in $\tau(u)$ is suppressed as that width increases.

The oscillations [1-3] represent motion along the path abcd in the τ-$\dot{\gamma}$ phase plane in the direction shown by the arrows in Fig. 1 if $\dot{\gamma} = 4UR^2a^{-3}$ lies between $\dot{\gamma}_1$ and $\dot{\gamma}_2$ (this rate is determined by U). This behavior can occur for an incompressible material only if very large cavities are formed in the capillary. A more reasonable hypothesis was proposed [1,2] when it was shown that the variation in $\dot{\gamma}$ during the oscillation is due to the compressibility of the polymer in the reservoir. Although the bulk strain is only 1-2% at pressures of ~100 atm (such as actually occur), this volume change in the reservoir may be comparable with the volume of the capillary.

The mass-balance equation for the system is

$$\int_{V(t)} \rho(\mathbf{x}, t)\,dv + \int_{v_0} \rho(\mathbf{x}, t)\,dv = \rho_0(V_0 + v_0) - \rho_0\int_0^t Q(\xi)\,d\xi. \qquad (2)$$

Here V(t) is the volume of polymer in the reservoir under the piston, $V_0 = \pi R^2 L$ is the initial volume under the piston, $v_0 = \pi a^2 l$ is the capillary volume, ρ_0 is the density of the polymer in the undeformed state (t = 0), and Q(t) is the polymer flow rate at the exit from the capillary. It is assumed that the polymer emerges with the density ρ_0.

The problem will subsequently be considered in the hydraulic approximation, the density distribution in the capillary being taken as the mean of ρ_0 and the density $\rho(t)$ in the reservoir; the spatial distribution of the density in the reservoir is also neglected. Then we get from (2) the approximate expression

$$\rho(t)\left(V(t) + \frac{v_0}{2}\right) \approx \rho_0\left(V_0 + \frac{v_0}{2}\right) - \rho_0\int_0^t Q(\xi)\,d\xi.$$

But $V(t) \gg v_0$ almost up to the end of the extrusion, and so we have

$$\rho(t)V(t) \approx \rho_0 V_0 - \rho_0\int_0^t Q(\xi)\,d\xi. \qquad (3)$$

We now restrict consideration to relaxation oscillations (fairly slow ones, as implied by [1-3]) and neglect all fast processes, as well as viscous friction in the reservoir, since the dissipation there is less than that in the capillary by orders of magnitude.

Further, we have

$$V(t) = V_0 - \pi R^2 Ut + Jp, \quad \varepsilon \equiv -1 + \rho(t)/\rho_0 = \beta p, \qquad (4)$$

Here J is the compliance of the reservoir walls and β is the compressibility of the polymer, which is about 10^{-10} cm^2/dyne for liquid

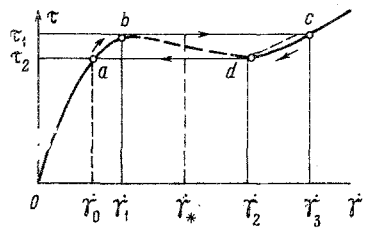

Fig. 1

*It has been asserted [4] that the falling section in Fig. 1 may be due to a falling section in $f(\tau)$, but this is incorrect. It is readily shown that such behavior in $f(\tau)$ leads to a region of hysteresis in $\dot{\gamma}(\tau)$, both branches of the hysteresis curve rising monotonically.

polymers (so $\varepsilon \ll 1$ at normal extrusion pressures) and which decreases as $1/T$ as T increases [8].

Then (3) and (4) give us a relation between p and Q, which we differentiate with respect to time and replace p and Q by τ and $\dot{\gamma}$ to get

$$\frac{d\tau}{dt} = \frac{\pi a^3}{4V_0}\frac{\tau_0(\dot{\gamma}_* - \dot{\gamma}) + \dot{\gamma}_*\tau}{1+\lambda - Ut/L},$$

$$\tau_0 = a(2l\beta)^{-1}, \quad \dot{\gamma} = 4Q(\pi a^3)^{-1},$$

$$\dot{\gamma}_* = 4UR^2a^{-3}, \quad \lambda = J\beta^{-1}V_0^{-1}. \tag{5}$$

Here the term quadratic in τ has been neglected as it contains the extremely small factor $J\beta$. If $\tau_0(\dot{\gamma}_* - \dot{\gamma}) \gg \dot{\gamma}_*\tau$, we have from (5) that

$$\frac{d\tau}{dt} \approx \frac{\pi a^3}{4V_0}\frac{\tau_0(\dot{\gamma}_* - \dot{\gamma})}{1+\lambda - Ut/L}. \tag{6}$$

This expression has been derived [6] from semiempirical considerations and has been used to find $d\tau/dt$ at the start of the cycles, which agreed to within 10% with the observed values.

To (5) we must add a rheological equation relating τ and $\dot{\gamma}$, which with the above approximations can be written as

$$\theta\frac{d\tau}{dt} + \tau = \varphi(\dot{\gamma}). \tag{7}$$

Equation (7) takes account of shear relaxation; in general, $\theta(\dot{\gamma})$. This equation will be applied to segments ab and cd (Fig. 1), so we approximate the relation as follows:

$$\theta(\dot{\gamma}) = \begin{cases}\theta_1 & (\dot{\gamma}_0 < \dot{\gamma} < \dot{\gamma}_1)\\ \theta_2 & (\dot{\gamma}_2 < \dot{\gamma} < \dot{\gamma}_3)\end{cases}. \tag{8}$$

Similarly, we approximate $\varphi(\dot{\gamma})$ on parts ab and cd by two straight lines:

$$\varphi(\dot{\gamma}) = \begin{cases}\eta_1(\dot{\gamma} - \dot{\gamma}_0) + \tau_2 & (\dot{\gamma}_0 < \dot{\gamma} < \dot{\gamma}_1)\\ \eta_2(\dot{\gamma} - \dot{\gamma}_2) + \tau_2 & (\dot{\gamma}_2 < \dot{\gamma} < \dot{\gamma}_3)\end{cases}$$

$$\left(\eta_1 = \frac{\tau_1 - \tau_2}{\dot{\gamma}_1 - \dot{\gamma}_0}, \quad \eta_2 = \frac{\tau_1 - \tau_2}{\dot{\gamma}_3 - \dot{\gamma}_2}\right). \tag{9}$$

We solve (7)–(9) for $\dot{\gamma}$ via the two-valued function $\varphi^{-1}(\dot{\gamma})$ and substitute the result into (5) to get equations for τ:

$$\left[\theta_k + \frac{4V_0\eta_k}{\pi a^3\tau_0}\left(1+\lambda - \frac{Ut}{L}\right)\right]\frac{d\tau}{dt} + \left(1 - \frac{\eta_k\dot{\gamma}_*}{\tau_0}\right)\tau =$$

$$= \eta_k(\dot{\gamma}_* - \dot{\gamma}_k) + \tau_2,$$

$$\eta_k = \begin{cases}\eta_1\\ \eta_2\end{cases}, \quad \dot{\gamma}_k = \begin{cases}\dot{\gamma}_0\\ \dot{\gamma}_2\end{cases}, \quad \theta_k = \begin{cases}\theta_1 & (\dot{\gamma}_0 < \dot{\gamma} < \dot{\gamma}_1)\\ \theta_2 & (\dot{\gamma}_2 < \dot{\gamma} < \dot{\gamma}_3)\end{cases}, \tag{10}$$

which describe $\tau(t)$ for motion on segments ab and cd in the τ-$\dot{\gamma}$ phase plane. In (10) we make allowance for the transient nature of the oscillatory motion.

Let the point in the τ-$\dot{\gamma}$ phase plane lie at a at time t_0 (Fig. 1). We introduce dimensionless variables and parameters:

$$\xi = \frac{t - t_0}{\theta_1}, \quad y = \frac{\tau}{\tau_2}, \quad y_0 = \frac{\tau_1}{\tau_2} > 1,$$

$$a_k = s_k + \frac{4V_0\eta_k s_k}{\pi a^3\theta_k\tau_0}\left(1 + \lambda - \frac{Ut_0}{L}\right)$$

$$b_k = \frac{4V_0\eta_k s_k U}{\pi a^3\tau_0 L}, \quad c_k = 1 - \frac{\eta_k\dot{\gamma}_*}{\tau_0}, \quad d_k = 1 + \frac{\eta_k}{\tau_2}(\dot{\gamma}_* - \dot{\gamma}_k)$$

$$s_1 = 1 \text{ (on ab)}, \qquad s_2 = \theta_2/\theta_1 \text{ (on cd)}, \tag{11}$$

where we have used the η_k, θ_k, and $\dot{\gamma}_k$ of (10); this enables us to write (10) in the form

$$(a_k - b_k\xi)\frac{dy}{d\xi} + c_k y = d_k. \tag{12}$$

Let $\zeta_n^{(1)}$ be the phase of cycle n corresponding to $y(\xi)$ increasing from $y = 1$ to $y = y_0$ (segment ab in Fig. 1), and let $\zeta_n^{(2)}$ be the phase of cycle n corresponding to $y(\xi)$ decreasing from $y = y_0$ to $y = 1$ (cd in Fig. 1); then $\zeta_n = \zeta_n^{(1)} + \zeta_n^{(2)}$ is the period of cycle n.

Let $y_n^{(1)}$ denote the rising part of $y_n(\xi)$ and $y_n^{(2)}$ the falling part in period n. Then we have the natural conditions

$$y_n^{(1)} = 1 \text{ for } \xi = \xi_{n-1} = \sum_{k=1}^{n-1}\zeta_k,$$

$$y_n^{(2)} = y_0 \text{ for } \xi = \xi_{n-1} + \zeta_n^{(1)} \quad (\xi_0 = 0), \tag{13}$$

and the solution to (12) that satisfies these is

$$y_n^{(1)} = \frac{d_1}{c_1} - \left(\frac{d_1}{c_1} - 1\right)\left(\frac{a_1 - b_1\xi}{a_1 - b_1\xi_{n-1}}\right)^{c_1/b_1},$$

$$\xi_{n-1} < \xi < \xi_{n-1} + \zeta_n^{(1)},$$

$$y_n^{(2)} = \frac{d_2}{c_2} + \left(y_0 - \frac{d_2}{c_2}\right)\left[\frac{a_2 - b_2\xi}{a_2 - b_2(\xi_{n-1} + \zeta_n^{(1)})}\right]^{c_2/b_2},$$

$$\xi_{n-1} + \zeta_n^{(1)} < \xi < \xi_n. \tag{14}$$

We always have $\tau_0 \gg \eta_k\dot{\gamma}_*$, if $\dot{\gamma}_1 < \dot{\gamma}_* < \dot{\gamma}_2$ in real viscometers of capillary type; then (11) implies that $c_k > 0$, and so (14) gives that for $y_n^{(1)}$ to rise we must have $d_1 > c_1$, which (11) shows is always the case. From the second formula in (14) we have that for $y_n^{(2)}$ to decrease we must have $y_n^{(2)}$. We substitute the y_0, c_2, and d_2 of (11) into this inequality to get an equivalent condition for decrease in $y_n^{(2)}$:

$$\dot{\gamma}_* < \dot{\gamma}_3(1 + \tau_1/\tau_0)^{-1}.$$

As $\tau_1 \ll \tau_0$ in a real capillary viscometer, the latter condition may be considered as obeyed if $\dot{\gamma}_1 < \dot{\gamma}_* < \dot{\gamma}_2$.

Then (13) and (14) give us a recurrence relation for the dimensionless phases of the oscillation:

$$\zeta_n^{(1)} = \left[1 - \left(\frac{d_1 - c_1y_0}{d_1 - c_1}\right)^{b_1/c_1}\right]\left(\frac{a_1}{b_1} - \sum_{k=1}^{n-1}\zeta_k\right),$$

$$\zeta_n^{(2)} = \left[1 - \left(\frac{c_2 - d_2}{c_2y_0 - d_2}\right)^{b_2/c_2}\right]\left(\frac{a_2}{b_2} - \sum_{k=1}^{n-1}\zeta_k - \zeta_n^{(1)}\right), \tag{15}$$

which shows that the period increases linearly with time, which agrees with experiment [2, 3]. The expression for the dimensionless period of cycle n is readily derived from (15) as

$$\zeta_{n+1} = \left(\frac{d_1 - c_1y_0}{d_1 - c_1}\right)^{nb_1/c_1}\left(\frac{c_2 - d_2}{c_2y_0 - d_2}\right)^{nb_2/c_2} \times$$

$$\times\left\{\frac{a_1}{b_1}\left[1 - \left(\frac{d_1 - c_1y_0}{d_1 - c_1}\right)^{b_1/c_1}\right]\left(\frac{c_2 - d_2}{c_2y_0 - d_2}\right)^{b_2/c_2} +\right.$$

$$\left. + \frac{a_2}{b_2}\left[1 - \left(\frac{c_2 - d_2}{c_2y_0 - d_2}\right)^{b_2/c_2}\right]\right\} \quad (n = 0, 1, 2, \ldots). \tag{16}$$

Consider now how the period is related to $\dot{\gamma}_*$, the nominal shear rate averaged over the capillary diameter. The piston in a real capillary apparatus moves very slowly, so the period varies only very slightly and is almost constant over a fairly long interval; this is so only when $b_k \ll 1$, so it is sufficient to consider the $\dot{\gamma}_*$ dependence of ζ_1 for b_1, $b_2 \ll 1$, for which we have

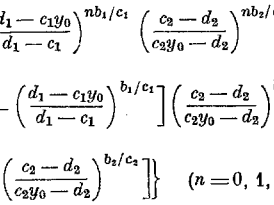

Fig. 2

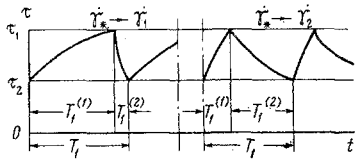

Fig. 3

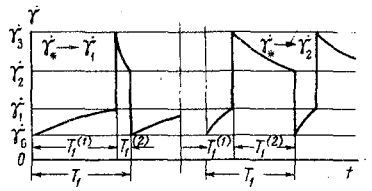

Fig. 4

$$\eta_k \gamma_k \tau_0^{-1} \ll 1, \quad c_k \approx 1, \quad U t_0 L^{-1} \ll 1.$$

Then we pass formally to the limit $b_k \to 0$ in the expression for ζ_1 in (16) and substitute for a_k and d_k from (11) with $c_k \to 1$ to get an approximate expression for the dimensional oscillation period $b_1 = \theta_1 \zeta_1$

$$T_1 \approx \left[\theta_1 + \frac{4V_0(\tau_1 - \tau_2)(1+\lambda)}{\pi a^3 (\gamma_1 - \gamma_0)\tau_0}\right] \ln \frac{\gamma_* - \gamma_0}{\gamma_* - \gamma_1} + \left[\theta_2 + \frac{4V_0(\tau_1 - \tau_2)(1+\lambda)}{\pi a^3 (\gamma_3 - \gamma_2)\tau_0}\right] \ln \frac{\gamma_3 - \gamma_*}{\gamma_2 - \gamma_*}. \quad (17)$$

Figure 2 shows the dependence of the circular frequency $\omega = 2\pi T_1^{-1}$ on $\dot{\gamma}_*$ implied by (17), which corresponds with experiment [2, 3] except at the end points $\dot{\gamma}_* = \dot{\gamma}_1$ and $\dot{\gamma}_* = \dot{\gamma}_2$, where (17) is not accurate and (16) should be used. The first term on the right in (17) is an approximate expression for the first phase $T_1^{(1)}$ of the cycle, while the second term is an expression for the second phase $T_1^{(2)}$. Then (17) implies that $T_1^{(1)}/T_1^{(2)}$ varies monotonically with $\dot{\gamma}_*$ in such a way that $T_1^{(1)} > T_1^{(2)}$ when $\dot{\gamma}_*$ is close to $\dot{\gamma}_1$ and $T_1^{(1)} < T_1^{(2)}$ when $\dot{\gamma}_*$ is close to $\dot{\gamma}_2$. This result also agrees entirely with the above experimental results.

Figures 3 and 4 show the general forms of $\tau(t)$ and $\dot{\gamma}(t)$ in the oscillation range $\dot{\gamma}_1 < \dot{\gamma}_* < \dot{\gamma}_2$; they agree entirely with the observed curves [2, 3].

There are no oscillations under these conditions (U = const) if $\dot{\gamma}_* < \dot{\gamma}_1$ or $\dot{\gamma}_* > \dot{\gamma}_2$; then (10) implies that $\tau(t)$ increases monotonically if $\dot{\gamma}_* < \dot{\gamma}_1$ or $\dot{\gamma}_* > \dot{\gamma}_3$, while if $\dot{\gamma}_2 < \dot{\gamma}_* < \dot{\gamma}_3$ there is one peak in $\tau(t)$ and the function passes over to a steady state for $t \to \infty$. This also agrees exactly with experiment [2].

Wall slip disrupts heat transfer to the capillary and may cause various secondary effects related to the structure of the melt (e.g., crystallization of rubber-like polymers by orientation near the wall); however, it has been shown [2] that these effects can be neglected to a few percent.

This theory completely confirms the hypothesis [2] as to the causes of oscillation for U = const; however, unstable flow conditions can occur also for p = const (in constant-pressure capillary viscometers). Here the instability cannot be described within the framework of this fairly crude theoretical scheme, and the causes of this form of instability remain an open question.

REFERENCES

1. J. M. Lupton, "Flow of polymer melts," Chem. Engng. Progr. Sympos. Ser., vol. 60, no. 49, 1964.

2. J. M. Lupton and J. W. Regester, "Melt flow of polyethylene at high rates," Polymer Engng. and Sci., vol. 5, no. 4, 1965.

3. R. W. Myerholtz, "Oscillating flow behavior of high-density polyethylene melts," J. Appl. Polymer Sci., vol. 11, no. 5, 1967.

4. J. P. Tordella, "Unstable flow of molten polymers: a second site of melt fracture," J. Appl. Polymer Sci., vol. 7, no. 7, 1963.

5. T. W. Huseby, "Hypothesis on a certain flow instability in polymer melts," Trans. Soc. Rheol., vol. 10, no. 1, 1966.

6. Yu. A. Buevich and A. I. Leonov, "Theory of dry friction of rubbery materials," PMTF [Journal of Applied Mechanics and Technical Physics], no. 6, 1965.

7. S. E. Bresler and B. L. Erusalimskii, The Physics and Chemistry of Macromolecules [in Russian], Nauka, Moscow-Leningrad, 1965.

8. E. Bernhardt, ed., Processing of Thermoplastic Materials [Russian translation], Goskhimizdat, Moscow, 1962.

21 November 1967 Moscow